J Therm Anal Calorim (2017) 130:2055–2067
DOI 10.1007/s10973-017-6508-9

Preparation of mesoporous silica-LDHs system and its coordinated flame-retardant effect on EVA

Yi Qian[1] · Shaoquan Li[1] · Xilei Chen[1]

Received: 13 September 2016 / Accepted: 25 May 2017 / Published online: 19 June 2017

Abstract This paper mainly studies synergistic flame-retardant effects and smoke suppression properties of mesoporous silica-LDHs system on the ethylene-vinyl acetate copolymer (EVA). The mesoporous silica-LDHs/EVA composites were prepared based on EVA as resin matrix, mesoporous silica-LDHs as flame-retardant composites. The flame-retardant and thermal degradation properties of the composites were characterized by limiting oxygen index (LOI), cone calorimeter test, scanning smoke density test (SDT), electronic microscopy (SEM) and thermogravimetry–Fourier transform infrared spectrometry (TG-IR) analysis. Remarkably, addition of certain amount of mesoporous silica-LDHs could evidently increase LOI values. The heat release rate and the total heat release of the composites were much lower than of pure EVA. The SDT results showed that the composites containing mesoporous silica-LDHs produced less smoke than pure EVA for a period of time. The morphologies and structures of the residues, revealed by SEM, ascertained that the formed char layers on the composites were denser than that of the LDHs/EVA composites. Mesoporous silica in the material can help smoke suppression. TG-IR data reveal that the incorporation of mesoporous silica-LDHs promoted the release of H_2O, and CO_2, meanwhile reduced harmful gases release.

Keywords Flame retardant · Ethylene-vinyl acetate · Mesoporous silica-LDHs · Smoke suppression · Thermal stability

✉ Yi Qian
qianyi1962@126.com

[1] College of Environment and Safety Engineering, Qingdao University of Science and Technology, Qingdao, Shandong 266042, People's Republic of China

Introduction

Mesoporous silica, a kind of pore structure material, has been widely used in investigation [1]. This is because this pore structure material has very high surface areas and easily functionalized surface that allow for binding to a great number of active sites within the framework of porous materials. Moreover, it also has large pores that can overcome the pore-diffusion limitation and in turn provide high-speed pathways for adsorbate molecules [2]. Previously, mesoporous silica is mainly used widely in molecular adsorption, storage, separation, catalysis and other aspects [3–6]. It also can serve as a drug carrier which can play a role in drug controlled release [7]. To date, several hundred reports along with some reviews have been published on the mesoporous silica in molecular adsorption. Up to now, still few people explore flammability about mesoporous silica which belongs a flame-retardant material. So it is very necessary for us to study the application of mesoporous silica in the fire retardant.

Layered double hydroxides (LDHs) are emerging as a new generation of flame-retardant material. LDHs have been shown to offer good flame retardancy and smoke suppression properties due to their unique chemical composition and layered structure. LDHs are two-nanostructured materials consisting of positively charged metal oxide/hydroxide layers and the interlayer exchangeable anions [8]. They are a class of anionic layered clays, whose general formula is $\left[M^{II}_{1-x}M^{III}_{x}(OH)_2\right]^{x+}\left[(Y^{m-})_{x/m}\right]\cdot nH_2O$, $\left[M^{II}_{1-x}M^{III}_{x}\ (OH)_2\right]^{x+}$ representing layer cation and $[(Y^{m-})_{x/m}]$ representing interlayer anion compositions, respectively, M^{II} is a divalent metal cation, M^{III} is a trivalent metal cation, and Y stands for *m* valence inorganic or organic acid anions [9]. LDHs can be prepared in a wide range of

compositions by coprecipitation of metal salts in alkaline medium at constant pH followed by a hydrothermal aging of the precipitate [10]. The LDH will absorb a large amount of heat during thermal decomposition and reduce the temperature of the combustion system. The released inert carbon dioxide and water vapor will dilute the concentration of combustible gas, which plays a gas-phase flame-retardant effect. Moreover, its special layer structure brings larger surface area and more surface adsorption activated centers, enabling it to adsorb volatile substance produced during the processing. The final pyrolysis residue, including magnesium and alumina oxide, will cover the polymer surface and form an insulation layer, which insulate from heat and oxygen in the air. As a flame retardant, LDHs have advantages like non-halogenated, non-toxic and no corrosive gas generation for polymer materials.

The ordered mesoporous silica intercalated into the LDHs structure; on the one hand, mesoporous particles fillers are highly attractive for the purpose which they can simultaneously improve the flammability and other properties of composites. On the other hand, the LDHs bring larger surface to adsorb a large number of mesoporous silica particles. The performance of mesoporous silica-LDHs hybrid materials will be perfect because performance of organic–inorganic component is complementary by cross-linking and compounding.

EVA is a transparent elastomeric material that exhibits some interesting properties, such as strong adhesion to glass substrate, low moisture absorption and low resin cost [11]. Consequently, EVA has been widely used in wire and cable, the films, hot melt adhesive, coating industries [12]. As pristine EVA is easily flammable because of its chemical composition, it is not suitable for many applications. To improve the flame retardant of this material, one general way is to fill additives into EVA.

In this paper, mesoporous silica was synthesized through sol–gel process using tetraethyl orthosilicate (TEOS) as silicon source. The mesoporous silica-LDHs composites were synthesized by coprecipitation method. Then, the flame-retardant and thermal properties of the mesoporous silica-LDHs/EVA composites were characterized by LOI, CCT, TG and TG-IR, respectively.

Experimental

Materials

EVA18 (containing 18 mass% vinylacetate) was bought from Beijing Eastern Petrochemical Co., Ltd. (China). Poly (ethylene glycol)-block-poly(propylene glycol)-block-poly (ethylene glycol) (P123) and 3-aminopropyltriethoxysilane (ATPES) were bought from Energy Chemical. Tetraethyl orthosilicate (TEOS) was bought from Tianjin Bodi chemical engineering Co., Ltd. (China). Other reagents were standard laboratory reagents and used as received without further purification.

Synthesis of mesoporous silica

As reported previously, mesoporous silica was prepared based on the sol–gel method [13]. In brief, in a typical synthesis, 62.20 mL of concentrated hydrochloric acid diluted to 1 L of hydrochloric acid solution made up in deionized water (0.75 mol L^{-1}). Afterward, 10.0 g of P123 was dissolved into 500 mL of diluted hydrochloric acid, and it was heated to 40 °C and stirred for 4 h. After complete dissolution, 20 mL of TEOS was then introduced dropwise to the mixture under intensive stirring. An hour later, 2.0 mL of APTES dispersed in a mixture of system, and the reaction was maintained at 40 °C for 24 h. Further, stop stirring crystallization at room temperature for 2 days. After suction filtering and washing to neutral with deionized water for several times, crude product was transferred into a muffle furnace to calcinate at 550 °C for 5 h. Mesoporous silica was obtained as white powder.

Synthesis of LDHs

Synthesis of Mg–Al LDHs

Mg–Al LDHs were prepared by the coprecipitation method at low supersaturation at 80 °C; the pH value was kept at 9–10. In detail, mixed $MgCl_2{\cdot}6H_2O$ and $AlCl_3{\cdot}6H_2O$ with M^{2+}/M^{3+} molar cationic ratio of 3.0/1.0 (solution A), preparing the solution of strong base which contained 0.5 mol L^{-1} Na_2CO_3, 1.5 mol L^{-1} NaOH (solution B). Then, solution A and solution B were added at a same speed to a beaker; the beaker provided with a mechanical stirrer and a water bath. The stirring speed was kept constant, and the temperature was 80 °C. Finally, the resulting product was filtered and washed thoroughly with deionized water until the pH reached 7. The sample was then dried in an oven at 80 °C until a constant mass was achieved.

Synthesis of mesoporous silica-LDHs

Mesoporous silica-LDHs can be produced by repeating the step like synthesis of Mg–Al LDHs. The mesoporous silica-LDHs were obtained by mixing mesoporous silica with LDHs. The only difference is that the mesoporous silica-LDHs materials were made by adding mesoporous silica into LDHs. That is to say, 0.0 g/0.5 g/1.0 g/1.5 g/2.0 g/2.5 g mesoporous silica were added to solution B (1L) before synthetic Mg–Al LDHs. So the samples were named LDH1 (containing 0.0 g mesoporous silica), LDH2 (containing 0.5 g mesoporous silica), LDH3 (containing 1.0 g

mesoporous silica), LDH4 (containing 1.5 g mesoporous silica), LDH5 (containing 2.0 g mesoporous silica) and LDH6 (containing 2.5 g mesoporous silica).

Preparation of mesoporous silica-LDHs/EVA composites

All composites were melt-compounded with a mixer at about 120 °C for 10 min. After mixing, the mixtures were then compression-molded at about 120 °C into sheets under a pressure of 10 MPa for 10 min. The sheets were cut into suitably sized specimens for fire testing. In this work, the additive level of all samples was 50%, and the samples were named ELDH0 (pure EVA), ELDH1 (containing 50% LDH1), ELDH2 (containing 50% LDH2), ELDH3 (containing 50% LDH3), ELDH4 (containing 50% LDH4), ELDH5 (containing 50% LDH5) and ELDH6 (containing 50% LDH6).

Characterization

BET surface area

BET is a kind of porous material test method of specific surface area and pore size distribution. The mixture of carrier gas (He) and adsorption gas (N_2) was continuously bubbled into the sample tube under a certain proportion so as to keep the balance of sample absorption at a low temperature. Single-point BET surface area measurements were taken using a Micromeritics Flowsorb II 2300 instrument.

X-ray diffraction (XRD)

XRD data were recorded at room temperature on a Philips X'Pert Pro Super apparatus (Nicolet Instrument Co., Madison, WI) using Cu Ka radiation with a nickel filter (wavelength = 1.5418Å) at a scan rate of 0.0167° s^{-1}.

Scanning electron microscopy (SEM)

The SEM studies were performed on the char residue using a Hitachi X650 scanning electron microscope.

Cone calorimeter test (CCT)

The CCT (Stanton Redcroft, UK) was performed according to ISO 5660 standard procedures. Each specimen of dimensions 100 × 100 × 4 mm^3 was wrapped in aluminum foil and exposed horizontally to an external heat flux of 50 kW m^{-2}.

Limiting oxygen index (LOI)

LOI was measured according to ASTM D 2863. The apparatus used was an HC-2 oxygen index meter (Jiangning Analysis Instrument Company, China). The specimens used for the test were of dimensions 100 × 6.5 × 3 mm^3.

Smoke density test (SDT)

A smoke density test machine JQMY-2 (Jianqiao Co, China) was used to measure the smoke characteristics according to ISO 5659-2(2006). Each specimen of dimensions 75 × 75 × 2.5 mm^3 was wrapped in aluminum foil and exposed horizontally to an external heat flux of 25 kW m^{-2} with or without the application of a pilot flame.

Thermogravimetry–Fourier transform infrared spectrometry (TG-IR)

The TG-IR instrument consists of a thermogravimeter (TG2009 F1, Netzsch Instruments, Germany), a Fourier transform infrared spectrometer (Vertex 70, Bruker Optics, Germany) and a transfer tube with an inner diameter of 1 mm connected to the TG and the infrared cell. The investigation was carried out from 30 to 800 °C at a linear heating rate of 10 K min^{-1} under the nitrogen flow rate of 3 × 10^{-5} m^3 min^{-1}.

Results and discussion

BET characterization of mesoporous silica

The textural properties of mesoporous silica were evaluated by BET. Figure 1 shows the nitrogen adsorption-desorption isotherms. The N_2 adsorption-desorption isotherms of mesoporous silica showed type IV character, which is typical of mesoporous material [13]. Furthermore, the sample exhibited three stages. The first stage is due to monolayer adsorption of nitrogen to the walls of the mesopores at a low relative pressure ($P/P_0 < 0.25$). The second stage is characterized by a steep increase in adsorption ($0.25 < P/P_0 < 0.4$). As the relative pressure increases, the isotherm exhibits a sharp inflection, characteristic of capillary condensation within the uniform mesopores. The third stage ($P/P_0 > 0.4$) in the adsorption isotherm is the gradual increase in volume with P/P_0, due to multilayer adsorption on the outer surface of the particles. Meanwhile, the pore size distributions (Fig. 2) showed a unique peak centered at about 3.4 nm diameter.

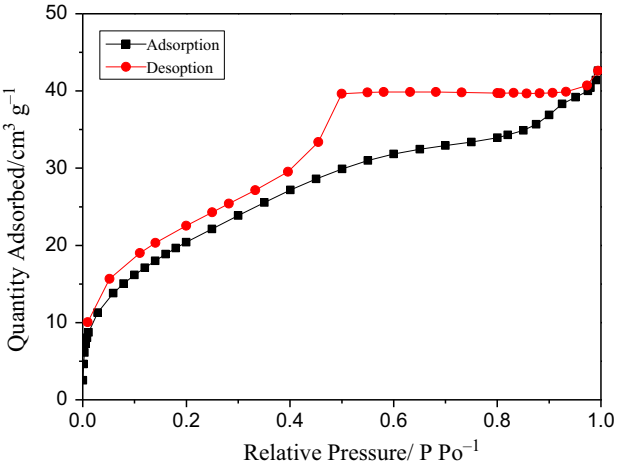

Fig. 1 Isotherm linear plot of mesoporous silica

SEM characterization of mesoporous silica

The structure and morphology of the materials were characterized using SEM. Figure 3 shows that the SEM photographs of mesoporous silica. As shown in Fig. 3a, mesoporous silica powder appears plenty of pore structure. Figure 3b shows the particle diameter of mesoporous silica varies from several nanometers to 20 nm. The results are fit to BJH Adsorption dV/dlog(D) Pore Volume of mesoporous silica.

XRD characterization of mesoporous silica-LDHs

XRD pattern of mesoporous silica-LDHs is shown in Fig. 4, and the lattice parameters are given in Table 1. The (003), (006), (009), (015), (110), (113) diffraction peaks of all sample are in good agreement with layered structures [14–16] and are ascribable to LDHs indexed by the JCPDS X-ray powder diffraction file of No. 38-0487. In general,

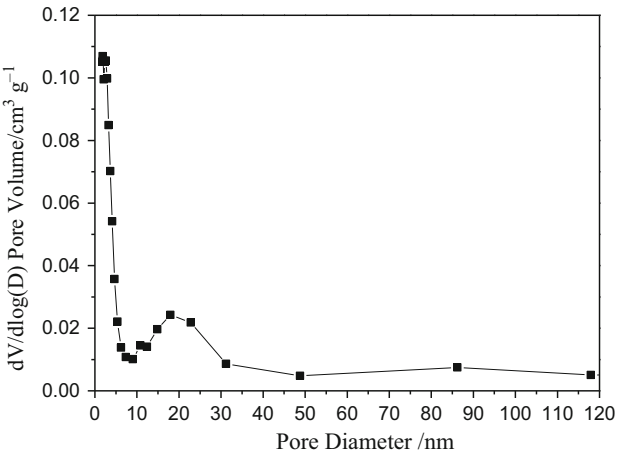

Fig. 2 BJH adsorption dV/dlog(D) pore volume of mesoporous silica

Fig. 4 shows that the diffraction peaks of all samples of mesoporous silica-LDHs are narrow and sharp and the baselines are low, indicating relatively well-formed crystallinity of LDHs; in low-angle region, 2θ values of (003), (006), (009) crystal planes have good multiple relationship, showing the LDHs synthesized have well crystalline layered structures; near 60°, diffraction peaks of (110) and (113) crystal planes are obviously separated, indicating that negative ions among layers have high degree of regularity, and the LDHs synthesized have good symmetry. At the same time, in connection with Table 1, $d_{(003)}$ of six samples is 0.774, 0.780, 0.786, 0.777, 0.784 and 0.779 nm, which indicates that negative ions of the LDHs synthesized among layers actually are carbonate radical.

Performance test of mesoporous silica-LDHs/EVA composites

CCT of mesoporous silica-LDHs/EVA composites

The cone calorimeter test is widely used for assessing the fire reaction behavior of polymer materials which is based on the oxygen consumption principle [17]. Although a cone calorimeter test is in a small scale, it can provide a wealth of information on the combustion behavior, especially the HRR and pHRR are often used to estimate combustion intensity as an important parameter. The obtained results have been found to correlate well with those obtained from a large-scale fire test and can be used to predict the combustion behavior of materials in a real fire [18, 19].

HRR of mesoporous silica-LDHs/EVA composites The HRR is a most important characteristic parameter for fire hazard [20]. It not only reflects the combustible gas heat generated by the decomposition of polymer, but also represents the heat released, which helps to judge the fire development and the threats to people [21, 22]. The HRR curves of the mesoporous silica-LDHs/EVA composites are shown in Fig. 5, and the correlated data are listed in Table 2. As is shown, the HRR curves of pure EVA (ELDH0) rise up quickly when ignite, and the pHRR was 1728.82 kW m^{-2}. When the 50 mass% LDH6 added to EVA (ELDH6), the curves show that the pHRR of the sample was 182.40 kW m^{-2}; the HRR of ELDH6 is the lowest among all samples. Figure 5 shows that all samples of HRR have declined when compared with pure EVA and ELDH1. So it could be concluded that an appropriate amount of mesoporous silica has certain effect on improvement in the flame retardancy. But along with the increase in mesoporous silica, the growing trend is not as tangible as before increasingly. On the other hand, the released inert carbon dioxide and water vapor will dilute the concentration of combustible gas; this charred layered

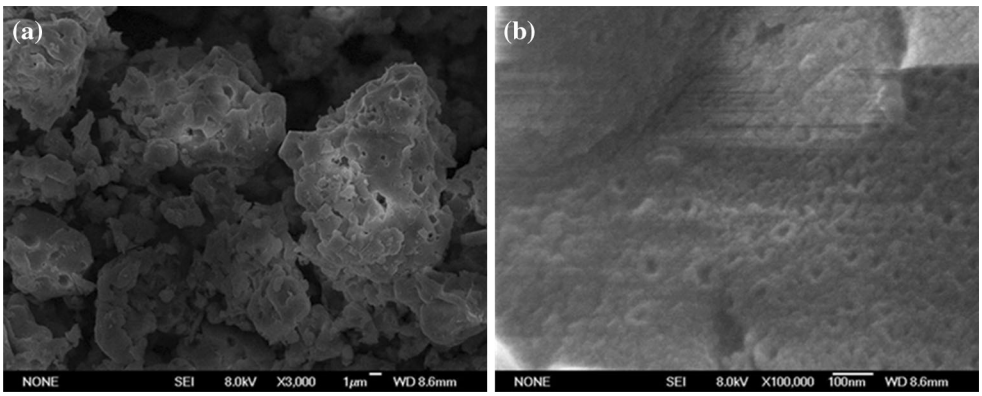

Fig. 3 SEM photographs of mesoporous silica

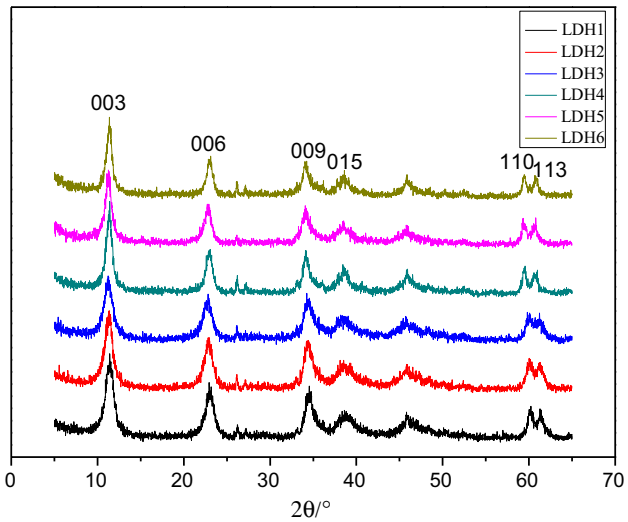

Fig. 4 XRD pattern of mesoporous silica-LDHs

Table 1 Structural parameters of mesoporous silica-LDHs

Sample code / nm	LDH1	LDH2	LDH3	LDH4	LDH5	LDH6
$d_{(003)}$	0.774	0.780	0.786	0.777	0.784	0.779
$d_{(006)}$	0.386	0.389	0.389	0.385	0.389	0.386
$d_{(009)}$	0.259	0.261	0.262	0.262	0.263	0.262
$d_{(015)}$	0.232	0.233	0.233	0.233	0.233	0.232
$d_{(110)}$	0.153	0.154	0.154	0.155	0.155	0.155
$d_{(113)}$	0.150	0.151	0.151	0.152	0.152	0.152
a	0.306	0.308	0.308	0.310	0.310	0.310
c	2.322	2.340	2.358	2.331	2.352	2.337

prevents heat transfer between the surface and the melting polymer. Thus, all mesoporous silica-LDH/EVA samples of HRR are reduced.

THR of mesoporous silica-LDHs/EVA composites Figure 6 presents the THR of all the samples. The slope of

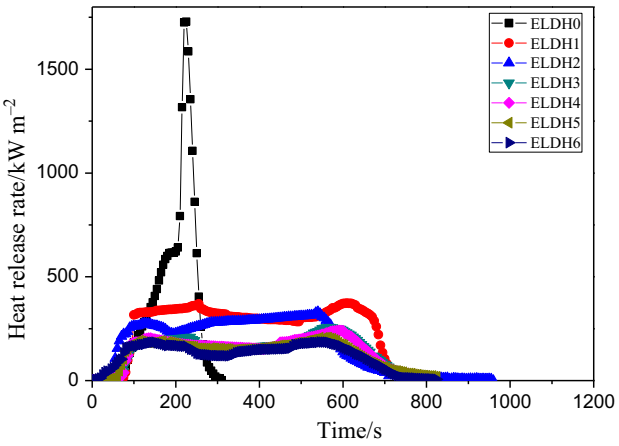

Fig. 5 HRR curves of all mesoporous silica-LDHs/EVA composites

Table 2 Data from cone calorimeter test

Sample code	PHRR/ kW m^{-2}	THR/ MJ m^{-2}	Time to pHRR/s	TTI/ s	Time to flame out/s
ELDH0	1728.82	191.47	225	44	294
ELDH1	368.74	179.86	620	48	758
ELDH2	330.46	163.67	555	56	715
ELDH3	249.77	118.49	580	66	754
ELDH4	236.03	115.05	600	61	735
ELDH5	201.84	111.14	575	66	752
ELDH6	182.40	107.99	560	60	741

THR curve can be assumed as representative of fire spread [23]. To a certain extent, THR only related to the internal energy of the material but independent of the environmental factors. From the chart known, ELDH0 (pure EVA) released the most heat in the combustion process, while the ELDH1 to ELDH6 has a decrease trend, which shows that the addition of mesoporous silica-LDHs can reduce the total heat releases. And from the slope of THR curve, the slope of ELDH6 is the most slow, indicating that the

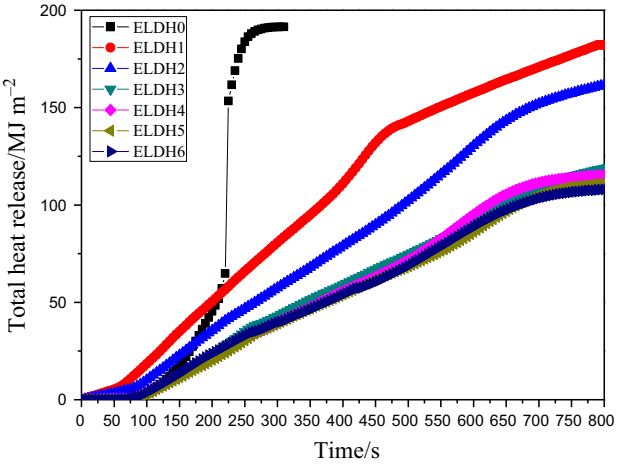

Fig. 6 THR curves of all mesoporous silica-LDHs/EVA composites

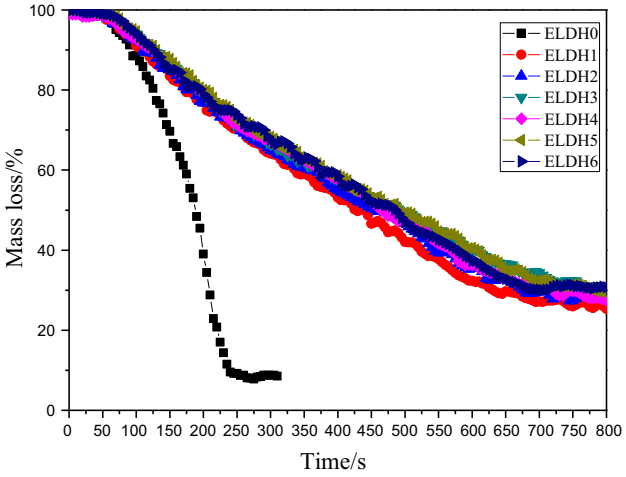

Fig. 7 Mass loss curves of all mesoporous silica-LDHs/EVA composites

Fig. 8 Photographs after cone calorimeter test

burning speed is slow. This further proved the flame-retardant effect of the mesoporous silica-LDHs/EVA composites. In addition, in the case of the same mesoporous silica-LDHs/EVA composites, the difference in the energy of the mesoporous silica-LDH/EVA composites with different contents is obviously different. At the same time, the LDH will absorb a large amount of heat during thermal decomposition and reduce the temperature of the combustion system. On the other hand, the final pyrolysis residue, including magnesium and alumina oxide, will cover the polymer surface and form an insulation layer, which insulate from heat and oxygen in the air, that is to say, the mesoporous silica-LDHs reducing the total heat release from the root.

Mass of mesoporous silica-LDHs/EVA composites The above seven samples of the dynamic curves of mass versus time are shown in Fig. 7. Figure 7 presents the mass variation of the char residue. The ELDH0 (pure EVA) was almost exhausted. The mass loss curve of ELDH1–ELDH6 tends to slow down, and residual mass of them are all above 30%, which shows mesoporous silica-LDHs improves the flame retardation of composite material. Join mesoporous silica-LDHs makes composite material burn more easily to produce char residue, which can isolate O_2 and heat transfer between burning areas and the bottom of the carbon layer; during combustion, a compact char residue may occur on the surface of the burning sample. The physical process of the char residue acts as a protective barrier [24].

Digital photographs of char residue Figure 8 shows the digital photographs of char residue of mesoporous silica-LDH/EVA composites. It can be seen that ELDH0 sample leaves no charred residues. However, the char residues of the ELDH1–ELDH6 samples are much integrated and compact. Such results are in good agreement with data of Fig. 7. As a kind of pore structure material, mesoporous silica has a strong adsorption and some of flame retardation. So it could increase the flame-retardant efficiency of materials and reduce the production of smoke. What is more, the mesoporous silica-LDHs can lead to the formation of compact layer on the sample surface. This means that the mesoporous silica-LDHs can improve the structures of the charred layers and reinforce thermal stability of the charred layers. The flame retardancy and smoke suppression of the composite materials has been improved. The photographs after cone calorimeter test results are well agreed with Figs. 6 and 7.

SEM of char residue Figure 9 shows the SEM photographs of the char residue after the combustion of ELDH1 with only Mg–Al LDHs and ELDH6 with mesoporous silica-LDHs/EVA at 50 kW m^{-2}. Obviously, the effective protection of the char layer can improve the flame retardant during combustion. As is symbolically depicted in the picture, we can notice that the surface of the ELDH1 is fragile and cracked. On the other hand, the char residue from ELDH6 shows a more tight structure. The compact char structure indicates mesoporous silica-LDH/EVA composites could prevent both heat and mass transfer between the flame zone and the materials, which is very important for EVA application. The SEM images also explained the flame-retardant performance of mesoporous silica-LDH/EVA composites in the cone calorimeter test.

SDT of mesoporous silica-LDHs/EVA composites

While the CCT results reflect the combustion behavior of the samples, the SDT gives a more detailed information about the smoke production which is very important to evaluate the smoke suppression character of the samples.

The SDT pattern obtained for the samples is shown in Fig. 10. The curve a (without flame) and curve b (with flame) both evidenced a sharp decline of pure EVA; finally the trend stabilized at a low level. A slower trend of SOD curve of ELDH1 can be seen which is compared to ELDH0 (pure EVA), indicating that LDH has smoke suppression properties. The curve of ELDH2–ELDH6 shows that the reduction rate is lower than of pure EVA, respectively. In the condition of no ignition, the SOD of ELDH6 stabilized at 90% above, which is better than of ELDH0 evidently. Figure 10b shows that ELDH2–ELDH6 was more than 80%, especially ELDH6, which is 95% above. It indicates that almost no smoke was spilled out during the burning process. As the quantity of mesoporous silica added to mesoporous silica-LDHs, the smoke suppression became increasingly apparent. LDH decomposes into Al_2O_3 and MgO when it was heated at a high temperature, those substances can prevent thermal transport and resistant air with inside material. This process changes the thermal decomposition pathways of polymers, which attributes to the cross-linking char formation. Al_2O_3 and MgO promote

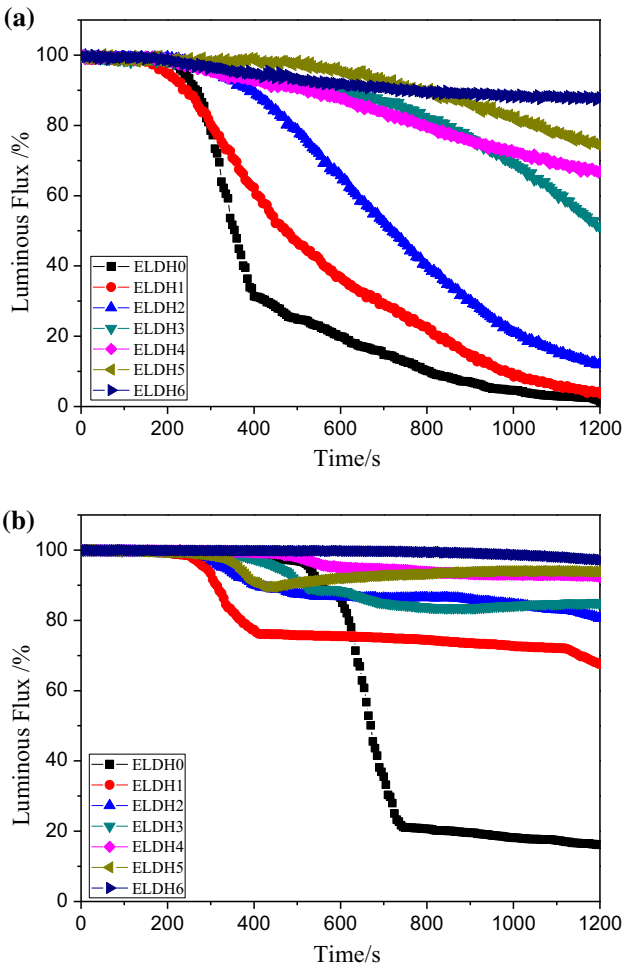

Fig. 10 SOD curves of all mesoporous silica-LDHs/EVA composites: **a** without and **b** with the application of the pilot flame

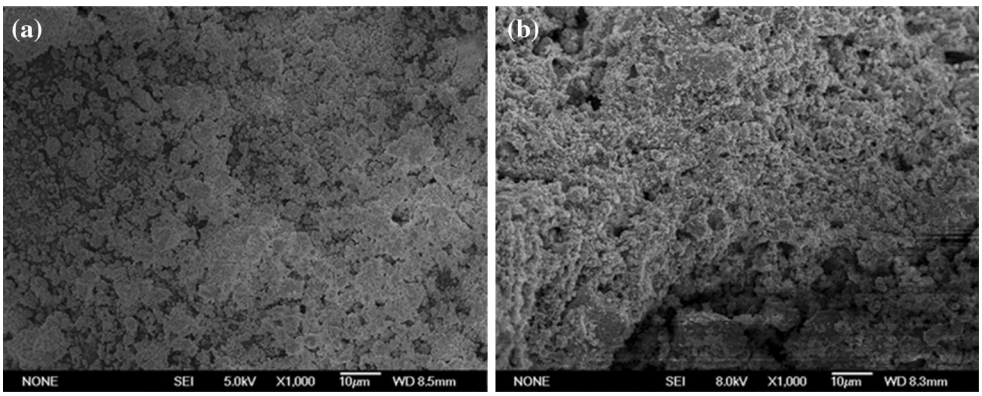

Fig. 9 SEM images of the outer surface of the char residue (A: ELDH1; B: ELDH6)

the formation of carbon layer and act as a polymer framework, which has smoke suppression. In addition, the giant-specific surface area and porous structure can give mesoporous materials useful characteristics such as high absorptive capacity which is good at absorbing smoke [25, 26].

LOI of mesoporous silica-LDHs/EVA composites

LOI test is a kind of simple and fast method to evaluate the flammability of polymer products, especially for screening flame-retardant formulations of polymers [27]. From Fig. 11, it is obvious that the LOI value of ELDH0 (pure EVA) is very low, which occupied only 19.8%. After entering 50% Mg–Al LDHs, it will rise to 27.0%, which means LDHs has flame-retardant effect to EVA. The LOI value of all mesoporous silica-LDH/EVA samples rises over 27.5% which shows mesoporous silica-LDH samples have ability to enhance flammability of composites. At the same time, with the increase in mesoporous silica in composite materials, the LOI value of ELDH2–ELDH6 will have an increase, after which descend. Among this mesoporous silica-LDH/EVA samples, the LOI value of ELDH4 was the highest and has reached 30.1%. During all tests, there are no dripping phenomenon happened with composite materials. It manifests that mesoporous silica-LDH composites can improve the anti-dripping properties of the flame retardant composites.

TG-IR characterization of mesoporous silica-LDHs/EVA composites

TG behavior of the mesoporous silica-LDHs/EVA composites The TG-IR analysis is always used to study the thermal degradation behavior of flame-retardant materials, and it also enables us to analyze the volatilized products at various temperatures. The results show in a thermogravimetric (TG) curve or its differential thermogravimetric (DTG) curve, and the Tmax of the sample is the maximum temperature of DTG curve [28]. Thus, TG can be used to study the thermal decomposition behavior of mesoporous silica-LDHs/EVA; at the same time, it can reflect the structural characteristics of matter to a certain extent. ELDH0–ELDH6's TG and DTG curves are shown in Fig. 12.

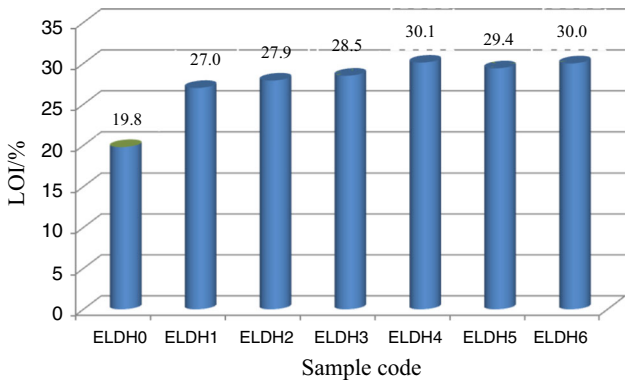

Fig. 11 LOI values for mesoporous silica-LDHs/EVA composites

Figure 12 shows the TG and DTG curves of all samples in a nitrogen atmosphere. Thermal stability of a polymeric material is extremely important when it comes to a flame retardant, which is mainly concerned about the release of decomposition products and the formation of the char [29].

The mass loss of the polymer is because volatilization of products generated by thermal decomposition was monitored as a function of a temperature ramp. The ELDH0 (pure EVA) in Fig. 12 underwent two degradation steps. The first decomposition step is caused by the loss of carboxylic acid and the formation of carbon–carbon double bonds along the polymer backbone between 300 and 400°C. The second step involved in random chain scission of the remaining material, forming unsaturated vapor species, e.g., butene and ethylene [30, 31]. There were three mass-loss steps for ELDH1–ELDH6. The first step was loss of the composites that is attributed to the loss of loosely bound water in the interlayer space of mesoporous silica-LDHs in the composites. The second and third steps belong to the simultaneous dehydroxylation and decarbonation of the acetate groups in EVA side chains and the scission of the main chains of EVA.

It is noted that ELDH1 assumed a lower decomposition rate in the third step and a higher one in the first and second steps than that of EVA. The incorporation of mesoporous silica-LDHs lowered the decomposition rate in the third step. It also accelerated the loss of carboxylic acid. When the temperature was higher than 700°C, the EVA sample left no residue and ELDH1–ELDH6 were left 30%. ELDH6, with both mesoporous silica and LDHs, exhibited higher thermal stability in all the degradation process than ELDH1. As a ternary composite, ELDH6 carried a better flame retardance than LDHs/EVA composites. This result confirms the synergistic effects. It also was ascertained by the above cone calorimeter results. Char morphology plays a more vital role in flame-retardant property than the quantity of a char, the same conclusion being found in Weil and Pate's study [32].

FTIR characterization of the mesoporous silica-LDHs/EVA composites Volatilized products of the composites during the thermal degradation were characterized by TG-IR technique as shown in Fig. 13. The evolved gas products for the three samples assumed characteristic bands in 3400–4000, 2800–3150, 2250–2400, 1700–1850, 1250–1500 and 950–1150 cm^{-1}, fitted to H_2O

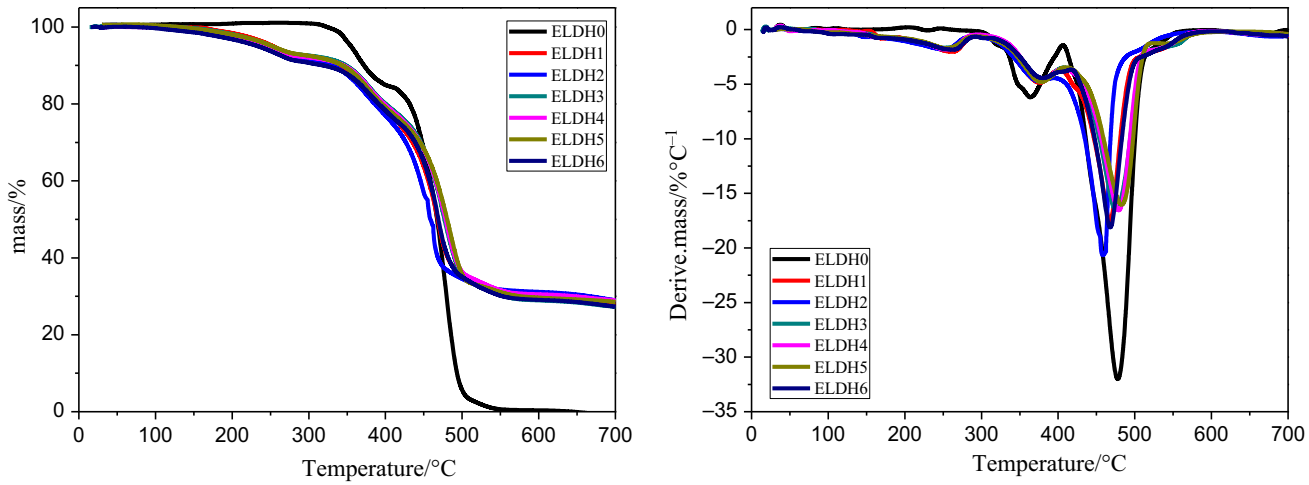

Fig. 12 TG and DTG curves of the samples

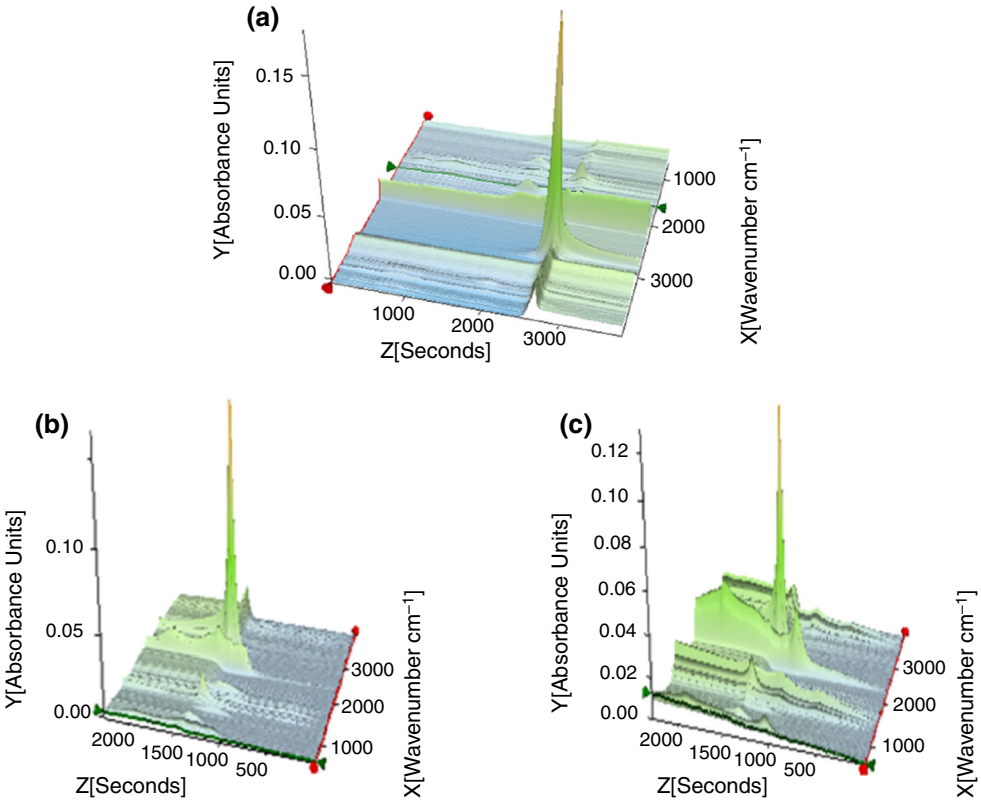

Fig. 13 3D TG-FTIR spectra of the pyrolysis products of **a** ELDH0, **b** ELDH1, and **c** ELDH6 during thermal degradation

(3400–4000 cm^{-1}), CO_2 (2300–2400 cm^{-1}), CO (2250–2300 cm^{-1}), carboxylic acid (1700–1850 cm^{-1}) and aliphatic hydrocarbons (2800–3150, 1250–1500 and 950–1150 cm^{-1}) [32–34], respectively. Depolymerization is known as a process associated with thermal degradation of polymers. The main decomposition products of the composites in this research were listed as above. In this study, the main decomposition of the composites is carboxylic acid, CO, CO_2 and aliphatic hydrocarbons.

It can be noticed that the depolymerization processes of the three samples were significantly different from their pyrolysis products after thermal degradation. The pure EVA sample decomposed drastically because it is flammable without any addition of flame retardants. It released large amount of carboxylic acids and aliphatic hydrocarbons in its decarboxylation and main chain breakdown. It is obvious that the decomposition of ELDH1 containing LDHs is slowed down. Furthermore, when mesoporous

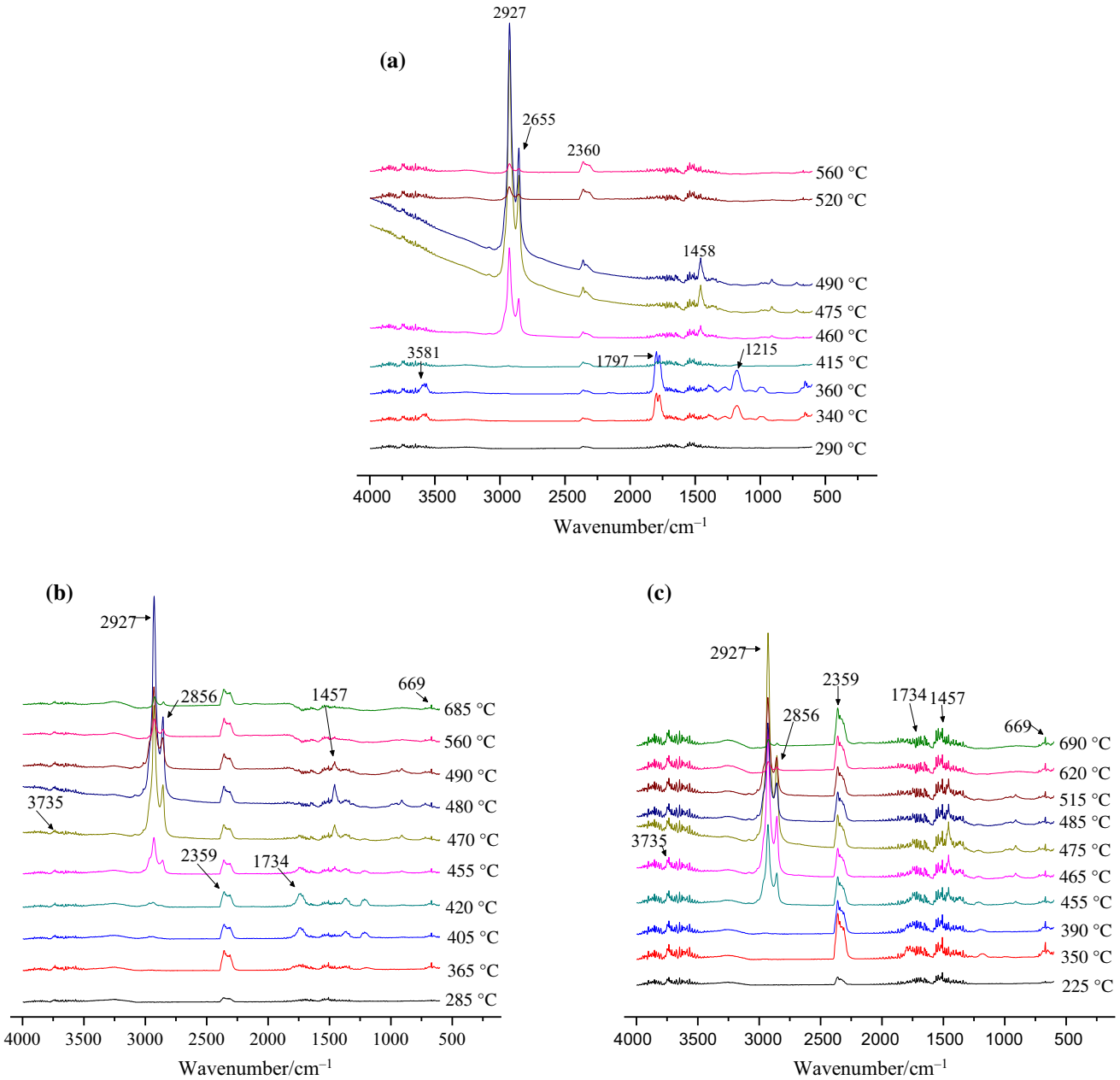

Fig. 14 FTIR spectra of pyrolysis products of **a** EVA, **b** ELDH1 and **c** ELDH6 at various temperatures

silica-LDHs are added into composites, the decomposition of ELDH6 is accelerated slightly more than that of ELDH1. The reasons for these phenomena will be discussed later.

The characteristic spectra obtained from 30 to 800°C are shown in Fig. 14. There were almost no infrared signals below 250°C, indicating no decomposition under that temperature. Beyond 250°C, the release of CO, CO_2 and H_2O could be detected. When the temperature was about 350°C, a maximum signal intensity at 1700–1850 cm^{-1}, reflecting evolution of carboxylic acid, can be observed. A maximum signal at 2800–3150 cm^{-1}, related to aliphatic hydrocarbons, appeared at 460°C. The signal intensity of the pyrolysis products declined gradually above 460°C, implying a slower decomposition rate of the mixture. The signals of ELDH1 and ELDH6 involving aliphatic hydrocarbons and carboxylic acid were less than of the pure EVA. More detailed information about the pyrolysis products of the composites is shown in Fig. 15.

Figure 15a shows that the release of H_2O for pure EVA shows two steps: the first step begins at about 330°C and reached its first peak at 370°C. The second step was above 500°C, the release of H_2O reaches a high level. Three steps can be observed from the process of water release for

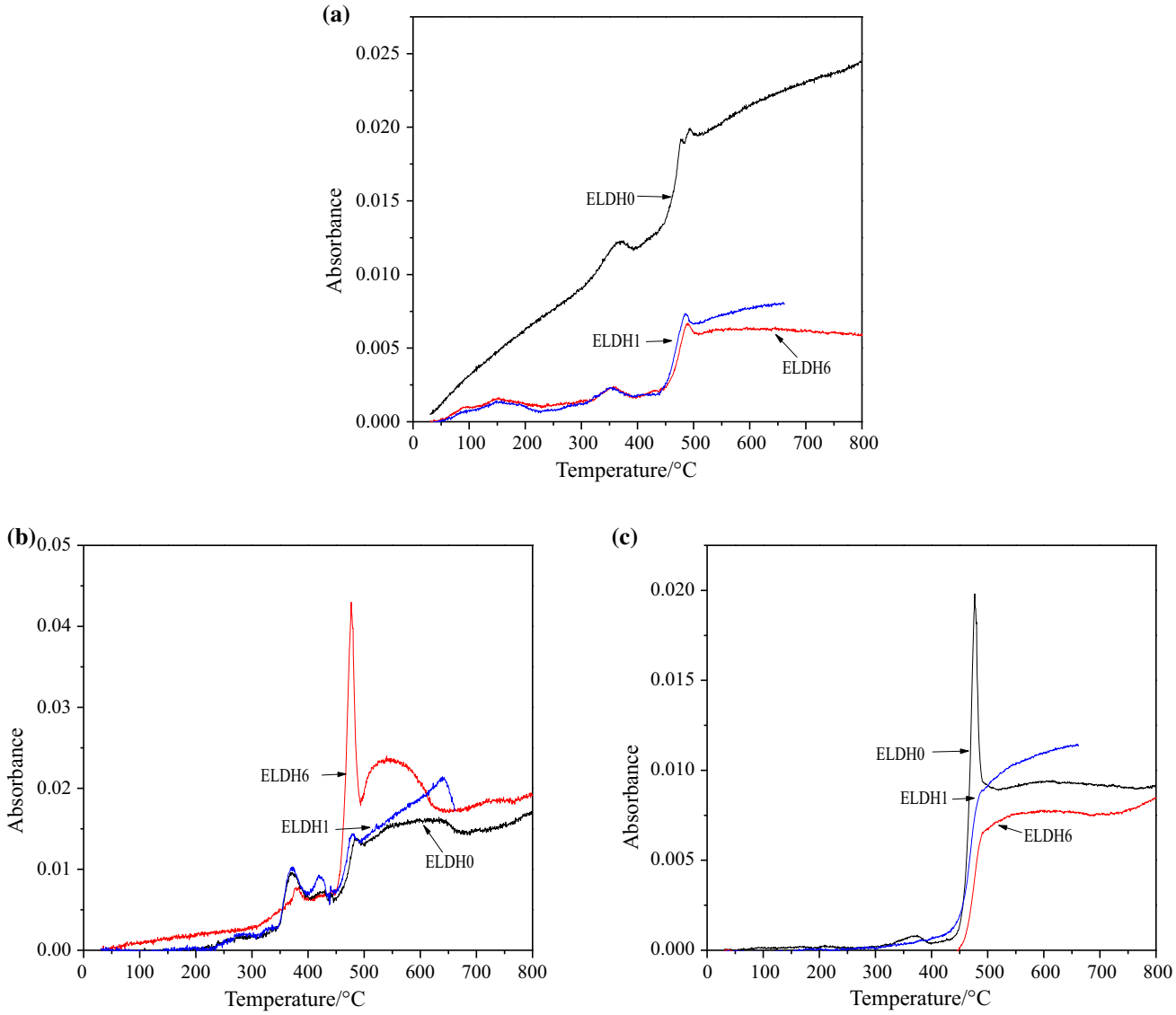

Fig. 15 Variation of **a** H_2O, **b** CO_2, **c** CO of the composites as a function of temperature cracking in nitrogen at 20 K min^{-1}

ELDH1 and ELDH6. It correlates well with the TG-DTG results. ELDH1 and ELDH6 evidently released less water than the pure EVA, and ELDH6 released the least water. When mesoporous silica was added into the composites, a char formed to protect the composites from burning, decomposition of EVA being slowed down.

As shown in Fig. 15b, no peak can be found in the release of CO_2 for the pure EVA until about 500°C, while a peak can be seen at about 370°C for both ELDH1 and ELDH6. The peak for ELDH1 and ELDH6 may be mainly caused by the CO_3^{2-} present in LDHs, while can be transformed into CO_2 when heated. The CO_2 releasing in ELDH6 was much less than that in ELDH1. The reason may be the formation of char on the surface of the composites which oxygen cannot reach the under substrate layer; thus, lots of CO is generated but not CO_2.

Figure 15c shows that when mesoporous silica-LDHs added into EVA, the release of CO is reduced significantly. The decrease in EVA may be the one reason for this, but the main reason may be the increase of the CO_2. The ternary composite ELDH6 produced least CO. It can be explained by more aliphatic hydrocarbons and carboxylic acid released from ELDH6 than from ELDH1 (Fig. 14). This phenomenon can be also illustrated by the incomplete combustion of the EVA leading by the lack of oxygen.

Conclusions

The LOI test shows that the addition of mesoporous silica-LDHs obviously increases the flame-retardant level of EVA. The flammability and smoke suppression

characteristics of mesoporous silica-LDHs/EVA composites had been compared with those of pure EVA and LDHs/EVA by LOI, CCT, SEM and SDT analysis. The data from CCT show that LDHs can significantly reduce the heat release during the combustion process. A moderate content of mesoporous silica-LDHs system can further reduce the value heat and smoke parameters. Furthermore, the mesoporous silica-LDHs system improves the structure of char residue, making it denser, tighter and containing many closed pores from digital photographs and SEM images. The SDT results showed that the mesoporous silica-LDHs/EVA composites produced less smoke than the LDHs/EVA composites and pure EVA.

It can be seen from TG-IR results that the mesoporous silica-LDHs/EVA composites can reduce flammable gases release at the thermal degradation process, and release CO_2 and H_2O as nonflammable gases at the initial time of thermal degradation. In a word, the TG-IR results indicated that the thermal stability of the mesoporous silica-LDHs/EVA composites was improved and the mechanism of the synergistic effects between LDHs and mesoporous silica may mainly depend on the condensed phase process.

Acknowledgements The authors gratefully acknowledge the National Natural Science Foundation of China (Grant No. 51372129), the National Natural Science Foundation of China (Grant No. 51572138) and the Projects of Science and Technology from Shandong Province (Grant No. 2013GSF11608).

References

1. Setyawan H, Yuwana M, Balgis R. PEG-templated mesoporous silicas using silicate precursor and their applications in desiccant dehumidification cooling systems. Microporous Mesoporous Mat. 2015;218:95–100.
2. Hao N, Tang F, Li L. MCM-41 mesoporous silica sheet with ordered perpendicular nanochannels for protein delivery and the assembly of Ag nanoparticles in catalytic applications. Microporous Mesoporous Mat. 2015;218:223–7.
3. Huang W, Yu X, Tang J, Zhu Y, Zhang Y, Li D. Enhanced adsorption of phosphate by flower-like mesoporous silica spheres loaded with lanthanum. Microporous Mesoporous Mat. 2015;217:225–32.
4. Wang H, Zhang SF, Liu JW, Ouyang LZ, Zhu M. Enhanced dehydrogenation of nanoscale MgH_2 confined by ordered mesoporous silica. Mater Chem Phys. 2012;136(1):146–50.
5. Park S, Bang J, Choi J. 3-Dimensionally disordered mesoporous silica (DMS)-containing mixed matrix membranes for CO_2 and non-CO_2 greenhouse gas separations. Sep Purif Technol. 2014;136:286–95.
6. Marcoux L, Florek J, Kleitz F. Critical assessment of the base catalysis properties of amino-functionalized mesoporous polymer-SBA-15 nanocomposites. Appl Catal A Gen. 2015;504:493–503.
7. Brunella V, Jadhav SA, Miletto I, Berlier G, Ugazio E, Sapino S. Hybrid drug carriers with temperature-controlled on–off release: a simple and reliable synthesis of PNIPAM-functionalized mesoporous silica nanoparticles. React Funct Polym. 2016;98:31–7.
8. Edenharter A, Breu J. Applying the flame retardant LDH as a Trojan horse for molecular flame retardants. Appl Clay Sci. 2015;114:603–8.
9. Li C, Wei M, Evans DG, Duan X. Recent advances for layered double hydroxides (LDHs) materials as catalysts applied in green aqueous media. Catal Today. 2015;247:163–9.
10. Gao Y, Wang Q, Wang J, Huang L, Yan X, Zhang X. Synthesis of highly efficient flame retardant high-density polyethylene nanocomposites with inorgano-layered double hydroxides as nanofiller using solvent mixing method. ACS Appl Mater Interface. 2014;6(7):5094–104.
11. Chen Y, Zou H, Liang M, Cao Y. Melting and crystallization behavior of partially miscible high density polyethylene/ethylene vinyl acetate copolymer (HDPE/EVA) blends. Thermochim Acta. 2014;586:1–8.
12. Sonia A, Dasan KP. Celluloses microfibers (CMF)/poly (ethylene-co-vinyl acetate)(EVA) composites for food packaging applications: a study based on barrier and biodegradation behavior. J Food Eng. 2013;118(1):78–89.
13. Rahman IA, Padavettan V. Synthesis of silica nanoparticles by sol-gel: size-dependent properties, surface modification, and applications in silica-polymer nanocomposites—a review. J Nanomater. 2012;11:8–22.
14. Ma J, Ding J, Li L, Zou J, Kong Y, Komarneni S. In situ reduction for synthesis of nano-sized Cu_2O particles on MgCuAl-LDH layers for degradation of orange II under visible light. Ceram Int. 2015;41(2):3191–6.
15. Prasanna SV, Kamath PV. Synthesis and characterization of arsenate-intercalated layered double hydroxides (LDHs): prospects for arsenic mineralization. J Colloid Interface Sci. 2009;331(2):439–45.
16. Tseng CH, Hsueh HB, Chen CY. Effect of reactive layered double hydroxides on the thermal and mechanical properties of LDHs/epoxy nanocomposites. Compos Sci Technol. 2007;67(11):2350–62.
17. Li L, Qian Y, Jiao CM. Synergistic flame retardant effect of melamine in ethylene–vinyl acetate/layered double hydroxides composites. J Therm Anal Calorim. 2013;114(1):45–55.
18. Liu J, Zhang Y, Peng S, Pan B, Lu C, Liu H. Fire property and charring behavior of high impact polystyrene containing expandable graphite and microencapsulated red phosphorus. Polym Degrad Stab. 2015;121:261–70.
19. Yi J, Yin H, Cai X. Effects of common synergistic agents on intumescent flame retardant polypropylene with a novel charring agent. J Therm Anal Calorim. 2013;111(1):725–34.
20. Wang J, Qian L, Xu B, Xi W, Liu X. Synthesis and characterization of aluminum poly-hexamethylenephosphinate and its flame-retardant application in epoxy resin. Polym Degrad Stab. 2015;122:8–17.
21. Jia CX, Chen XL, Qian Y. Synergistic flame retardant effect of graphite powder in EVA/LDH composites. Plast Rubber Compos. 2014;43(2):46–53.
22. Xu MJ, Xu GR, Leng Y, Li B. Synthesis of a novel flame retardant based on cyclotriphosphazene and DOPO groups and its application in epoxy resins. Polym Degrad Stab. 2016;123:105–14.
23. Qian Y, Wei P, Jiang P, Li Z, Yan Y, Ji K. Aluminated mesoporous silica as novel high-effective flame retardant in polylactide. Compos Sci Technol. 2013;82:1–7.
24. Liu L, Hu J, Zhuo J, Jiao C, Chen X, Li S. Synergistic flame retardant effects between hollow glass microspheres and magnesium hydroxide in ethylene-vinyl acetate composites. Polym Degrad Stab. 2014;104:87–94.
25. Chen X, Jiang Y, Jiao C. Smoke suppression properties of ferrite yellow on flame retardant thermoplastic polyurethane based on ammonium polyphosphate. J Hazard Mater. 2014;266:114–21.

26. Hu W, Yu B, Jiang SD, Song L, Hu Y. Hyper-branched polymer grafting graphene oxide as an effective flame retardant and smoke suppressant for polystyrene. J Hazard Mater. 2015;300:58–66.
27. Li L, Qian Y, Jiao CM. Influence of red phosphorus on the flame-retardant properties of ethylene vinyl acetate/layered double hydroxides composites. Iran Polym J. 2012;21(9):557–68.
28. Hirose S, Kobashigawa K, Izuta Y, Hatakeyama H. Thermal degradation of polyurethanes containing lignin studied by TG-FTIR. Polym Int. 1998;47(3):247–56.
29. Salgado J, Paz-Andrade MI. The effect of firesorb as a fire retardant on the thermal properties of a heated soil. J Therm Anal Calorim. 2009;95(3):837–42.
30. Zhao CX, Liu Y, Wang DY, Wang YZ. Synergistic effect of ammonium polyphosphate and layered double hydroxide on flame retardant properties of poly(vinyl alcohol). Polym Degrad Stab. 2008;93(7):1323–31.
31. Zanetti M, Kashiwagi T, Falqui L, Camino G. Cone calorimeter combustion and gasification studies of polymer layered silicate nanocomposites. Chem Mater. 2002;14(2):881–7.
32. Weil ED, Patel NG. Iron compounds in non-halogen flame-retardant polyamide systems. Polym Degrad Stab. 2003;82(2):291–6.
33. Gregoriou VG, Kandilioti G, Bollas ST. Chain conformational transformations in syndiotactic polypropylene/layered silicate nanocomposites during mechanical elongation and thermal treatment. Polymer. 2005;46(25):11340–50.
34. Chen YJ, Zhan J, Zhang P, Nie SB, Lu HD, Song L, Hu Y. Preparation of intumescent flame retardant poly(butylene succinate) using fumed silica as synergistic agent. Ind Eng Chem Res. 2010;49(17):8200–8.